# Primordial black holes from high peaks in the density field

Author: Judith Cid Giménez
*Facultat de Física, Universitat de Barcelona, Diagonal 645, 08028 Barcelona, Spain.**

Advisor: Jaume Garriga

**Abstract:** In this work we study the formation of primordial black holes, through the collapse of spherically symmetric overdensities during the radiation era. We study the effect of departures from Gaussianity of the primordial curvature perturbations in the threshold for collapse of high peaks. We find that non-Gaussianity can affect the probability of black hole formation significantly.

## I. INTRODUCTION

Primordial Black Holes (PBH) may have formed during the radiation dominated era due to unusually high peaks in a nearly-Gaussian distribution of cosmological density perturbations. [1, 2] There are strong observational constraints on the abundance of PBH over a wide range of mass scales. Nonetheless, these still allow for several phenomenologically interesting possibilities. For instance, PBH of sublunar or stellar mass may constitute a sizable fraction of all dark matter in the universe. Also, the origin of supermassive black holes at the center of galaxies is not very well understood at present, and one possibility is that they may have formed by accretion from a smaller intermediate mass PBH seed [3].

It is customary to characterize perturbations to the homogeneous Friedmann-Robertson-Walker (FRW) universe by using the so-called gauge-invariant curvature perturbation $\zeta(\vec{x}, t)$ [see Eq. (11) below]. An important property of this variable is that it stays constant in time $\zeta \approx \zeta(\vec{x})$ on superhorizon scales, while the wavelength of the perturbation is still larger than the Hubble radius. PBH will form if perturbations are sufficiently large ($\zeta \sim 1$) at the moment of re-entering the cosmological horizon, otherwise they will simply dissipate into pressure waves. Hence, in order for the PBH to be produced in significant abundance, the power spectrum (or variance) $P_\zeta(k)$ of cosmological perturbations (of wavenumber $k$) has to have a significant amplitude at the comoving scale corresponding to the size of the PBH. The power spectrum is thought to be determined by inflationary dynamics in the early universe. Observationally, the power spectrum is known to be very small $P_\zeta \sim 10^{-9}$ and nearly scale invariant on cosmological scales, ranging from the scale of the current Hubble radius down to the galactic scale. However, certain inflationary models [4] can produce the necessary enhancement $P_\zeta \sim 10^{-2}$ to form PBH at much smaller scales. Some of these models also give a specific type of non-Gaussianity in the distribution of $\zeta$, which is called local non-Gaussianity, which may have some effect in the probability of PBH formation.

A question of practical interest in cosmology is to determine the abundance of PBH in a given scenario. A useful estimator for the strength of a spherically symmetric perturbation is the so-called compaction function $\mathcal{C}[\zeta(r)]$. This is an average of the density perturbation over a region of size $r$. Denoting by $r_m$ the maximum of this function, the idea is that a PBH will form if the optimized compaction function $\mathcal{C}[\zeta(r_m)]$ exceeds a certain threshold $\mathcal{C}_{th}$ [5]. The precise threshold value $\mathcal{C}_{th} \sim 1$ actually depends on the specific profile of the spherically symmetric perturbation, and can be found through numerical simulation.

In this work we perform a numerical simulation of primordial black hole formation, with initial conditions motivated by inflationary models [4] where the power spectrum has a very sharp enhancement at the PBH scale. We model such enhancement by a $\delta$ function in momentum space. In this case, the high peaks of the random field $\zeta(r)$ have a typical profile which is nearly spherically symmetric and which can be given analytically in terms of elementary functions, even if we include the effect of local non-Gaussianity [4].

We will use numerical simulations in order to determine the corresponding threshold value $\mathcal{C}_{th}$. The formation of the black hole for a given initial condition can be inferred from the behaviour of perturbations which do not dissipate after entering the horizon but continue growing until a trapped surface [6] is formed. This signals the onset of gravitational collapse. Furthermore, we will analyse the effect of a small local non-Gaussianity on the value of $\mathcal{C}_{th}$.

To implement the simulation we have used A. Escrivà's code [7], which uses spectral methods in order to solve the Misner-Sharp (MS) partial differential equations [8] for spherically symmetric gravitational collapse. The code is able to provide values of $\mathcal{C}_{th}$ with accuracy of order $10^{-3}$ in a very short time-scale, of the order of a few minutes on a laptop computer. This is in contrast with other existing codes based on adaptive mesh refinement, which require a much longer time-scale for each run. The original code was developed in a slightly different gauge than we will use, so we have introduced a small modification in order to use the curvature perturbation $\zeta$ as our input for initial conditions.

The plan of the paper is the following. In Section II, we present the Misner-Sharp equations for spherically symmetric spacetimes. In Section III, the long wavelength

*Electronic address: jcidgime7@alumnes.ub.edu

approximation is introduced to implement initial conditions. In section IV, we particularize the typical shape of a high peak in the curvature perturbation profile and we introduce local non-Gaussianity. In section V, the criteria which determine the formation of PBH are explained. The results are presented in section VI. Our conclusions are summarized in Section VII.

## II. THE MISNER-SHARP EQUATIONS

The Misner-Sharp equations (MS) are the Einstein's equations for a spherically symmetric spacetime, in a frame comoving with an ideal fluid [8]. In this case, the metric can be written in the general diagonal form

$$ds^2 = -A(r,t)^2dt^2 + B(r,t)^2dr^2 + R(r,t)^2d\Omega^2 \quad (1)$$

where $d\Omega = d\theta^2 + \sin^2\theta d\phi^2$ is the metric on the unit 2-sphere, and with the radial coordinate $r$ moving along with the fluid. The metric components $A(r,t)$, $B(r,t)$ and $R(r,t)$ are all positive, the latter one corresponding to the areal radius of the 2-spheres. Following [8], the proper-time and radial proper distance derivatives are defined as

$$D_t \equiv \frac{1}{A}\frac{\partial}{\partial t} \quad \text{and} \quad D_r \equiv \frac{1}{B}\frac{\partial}{\partial r}. \quad (2)$$

Applying the last two operators to $R$ we can also define

$$U \equiv D_t R = \frac{1}{A}\frac{\partial R}{\partial t} \quad \text{and} \quad \Gamma \equiv D_r R \equiv \frac{1}{B}\frac{\partial R}{\partial r}. \quad (3)$$

We may now introduce the Misner-Sharp mass $M(r,t)$ through the equation

$$\Gamma^2 - U^2 = 1 - \frac{2M}{R}. \quad (4)$$

We will also use the form of the stress energy tensor of an ideal fluid

$$T^{\mu\nu} = (p+\rho)u^\mu u^\nu + pg^{\mu\nu} \quad (5)$$

where $u^\mu$ is the four-velocity field of the fluid, $\rho$ is the internal energy density of the fluid, and $p$ is the pressure. The fluid is at rest in comoving coordinates. During the radiation era, the equation of state is $p = \frac{1}{3}\rho$.

In terms of these variables, the MS equations take the form

$$D_t U = -\frac{\Gamma}{\rho+p}D_r p - \frac{M}{R^2} - 4\pi R p, \quad (6)$$

$$D_t \rho = -\frac{\rho+p}{\Gamma R^2}D_r(R^2 U), \quad (7)$$

$$D_r A = -\frac{A}{\rho+p}D_r p, \quad (8)$$

$$D_r M = 4\pi R^2 \Gamma \rho. \quad (9)$$

We may now discuss the issue of initial conditions.

## III. THE LONG WAVELENGTH APPROXIMATION AND INITIAL CONDITIONS

Initially, at early times, perturbations have a physical wave-length $L$ much larger than the Hubble radius $H^{-1}$. Hence, we are going to consider the long wavelength approximation to determine the form of our initial metric and hydrodynamical variables. This is based in expanding the exact solutions in a power series of a parameter

$$\epsilon(t) \equiv \frac{1}{H(t)L(t)}, \quad (10)$$

to the lowest non-vanishing order in $\epsilon(t) \ll 1$.

In the limit $\epsilon \to 0$, the metric of a perturbed FRW model takes the form [9]

$$ds^2 = -dt^2 + a^2(t)e^{2\zeta(r)}(dr^2 + r^2 d\Omega^2). \quad (11)$$

This is written in a coordinate system where the energy density of the fluid is used as a clock, so that $t = const.$ surfaces coincide with $\rho = const.$ surfaces in the long wavelength limit. He have also restricted to spherical symmetry, which excludes the presence of tensor modes (gravitational waves).

In Ref. [7], the metric

$$ds^2 = -dt^2 + a^2(t)\left[\frac{d\hat{r}^2}{1-K(\hat{r})\hat{r}^2} + \hat{r}^2 d\Omega^2\right] \quad (12)$$

is used instead of Eq. (11). Both are related by the coordinate transformation $\hat{r} = re^{\zeta(r)}$, $(1-K(\hat{r})\hat{r}^2)^{-1/2}d\hat{r} = e^{\zeta(r)}dr$. We have used this transformation in order to write the explicit long wavelength approximate solutions of the Misner-Sharp equations, which were originally expressed in terms of $K(\hat{r})$ in [7, 10].

In terms of $\zeta(r)$, we have

$$A = 1 + \epsilon^2\tilde{A} = 1 + \epsilon^2 - \frac{1}{4}\tilde{\rho},$$

$$R = a(t)e^{\zeta(r)}r(1+\epsilon^2\tilde{R}) = a(t)e^{\zeta(r)}r(1+\epsilon^2 - \frac{1}{8}\tilde{\rho} + \frac{1}{2}\tilde{U}),$$

$$\rho = \frac{3}{8\pi}H^2(t)(1+\epsilon^2\tilde{\rho}),$$

$$U = H(t)R(1+\epsilon^2\tilde{U}),$$

$$M = \frac{4\pi}{3}\rho R^3(1+\epsilon^2\tilde{M}) = \frac{4\pi}{3}\rho R^3(1+\epsilon^2 - 4\tilde{U}),$$

where the tilde variables are the explicit expressions of the perturbation. The functions $\tilde{\rho}$ and $\tilde{U}$ represent the energy density and velocity perturbation, given by

$$\tilde{\rho} = -\frac{4}{9}\frac{e^{2\zeta(r_k)}}{e^{2\zeta(r)}}r_k^2\Bigg[(\zeta''(r) + \zeta'(r)\left(\frac{3}{r} - \frac{1}{r(1+r\zeta'(r))} + \zeta'(r)\left(\frac{1}{2} - \frac{1}{1+r\zeta'(r)}\right)\right)\Bigg],$$

$$\tilde{U} = -\frac{1}{6}\frac{e^{2\zeta(r_k)}}{e^{2\zeta(r)}}\zeta'(r)\left[\frac{2}{r} + \zeta'(r)\right]r_k^2.$$

where $r_k$ is the comoving lengthscale of the perturbation associated to the wavenumber k, i.e. $r_k e^{\zeta(r_k)} = 1/H(t)a(t)\epsilon$.

## IV. THE TYPICAL HIGH PEAK PROFILE

Quantum fluctuations in an inflationary phase of the very early universe yield inhomogeneites $\zeta(\vec{x})$ which can be treated as a random field. A random field can be thought of as an infinite set of random variables $\zeta_{\vec{k}}$, one for each Fourier mode $\vec{k}$. Such variables are nearly-Gaussian distributed. In the Gaussian case, the distribution is fully determined by the variance $\sigma(k)$, or equivalently, by the dimensionless power spectrum,

$$P_\zeta(k) \equiv \frac{\sigma^2 k^3}{2\pi^2}. \tag{13}$$

which characterizes the variance of the random field per logarithmic interval in $k$. The peaks of a Gaussian random field have a mean profile that depends on the spatial two-point correlation function of $\zeta(\vec{x})$ [11]

$$\psi(r) \equiv \frac{1}{\sigma_0^2}\langle\zeta(r)\zeta(0)\rangle = \frac{1}{\sigma_0^2}\int P_\zeta(k)\,\mathrm{sinc}\,kr\,\frac{dk}{k} \tag{14}$$

where $\sigma_0^2 \equiv \int \frac{dk}{k} P_\zeta(k)$ is a normalization factor such that $\psi(0) = 1$. We are interested in high peaks, whose typical profile is approximately given by [11]

$$\zeta(r) = \mu\psi(r) + O(\sigma_0) \tag{15}$$

with an amplitude $\mu \gg \sigma_0$. As mentioned in the introduction, we are going to consider an idealized form for the enhancement in the power spectrum at the PBH scale $k_0$, given by a delta function, i.e.

$$P(k) = \sigma_0^2 k_0 \delta(k - k_0). \tag{16}$$

In this case, the typical shape of a high peak is given by

$$\zeta(r) = \mu\,\mathrm{sinc}(k_0 r). \tag{17}$$

In realistic scenarios $\sigma_0 \sim 10^{-1}$ [3], while PBH are produced by rare non-linear perturbations with $\mu \sim 1$.

So far, we have assumed that the primordial curvature perturbation is given by a Gaussian random field, but as mentioned in the introduction it is also interesting to consider the effect of a small local-type non-Gaussianity. This feature is usually present in models with a sharp enhancement of the power spectrum at small scales. If the non-Gaussianity is small, the curvature perturbation $\zeta$ can be parametrized as

$$\zeta(\vec{x}) = \zeta_G(\vec{x}) + f_{NL}\zeta_G^2(\vec{x}), \tag{18}$$

where $\zeta_G$ is a fictitious Gaussian distributed random variable, and we have introduced the non-Gaussianity parameter $f_{NL}$.

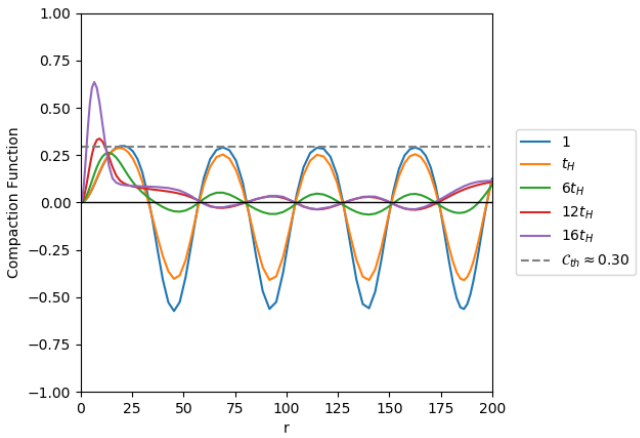


FIG. 1: In this figure we show the compaction function $\mathcal{C}(r)$ of the Gaussian profile with $\mu = 0.64$ for different moments in time. $\mathcal{C}$ is dimensionless, $r$ is in units of $t_i$ and time is in terms of the horizon crossing time $t_H$ which is also in terms of $t_i$. The threshold value $\mathcal{C}_{th}$ of the compaction function is also shown as a dashed grey horizontal line.

## V. THE CRITERION

Assuming spherical symmetry we can introduce the compaction function $\mathcal{C}$ [5] as the mass excess relative to the FRW background $M_b$, divided by the areal radius [5]

$$\mathcal{C} \equiv \frac{M(r,t) - M_b(r,t)}{R(r,t)}. \tag{19}$$

In the long wavelength limit, the compaction function is time independent, and can be expressed in terms of the curvature perturbation as

$$\mathcal{C}(r) = \frac{1}{3}(1 - (1 + r\zeta'(r))^2), \tag{20}$$

where the prime denotes the partial derivative with respect to the radial coordinate.

It turns out that $\mathcal{C}$ is a very useful estimator of the strength of a perturbation. In particular, if the initial $\mathcal{C}(r)$ has a maximum at $r = r_m$ which satisfies $\mathcal{C}(r_m) > \mathcal{C}_{th}$, then a PBH will be formed after $R(r_m, t)$ enters the horizon [5]. From Eq. (20) it is easy to see that $\mathcal{C}_{th}$ cannot be larger than 1/3. Also, it has been argued that $\mathcal{C}_{th}$ cannot be smaller than 0.21 [12], so the threshold must lie in the range

$$0.21 \leq \mathcal{C}_{th} \leq 1/3. \tag{21}$$

The precise value of $\mathcal{C}_{th}$ depends on the profile of the initial perturbation, and we will find it for our model by the use of numerical simulations. The criterion for formation of a PBH is that a trapped surface is formed during the evolution of the overdensity. This implies that a singularity will form to the future of the trapped surface [6], and thus signals the onset of gravitational collapse.

To identify the trapped surfaces, we consider the expansion $\Theta \equiv \nabla_\mu k^\mu$ of null geodesic congruences $k^\mu$ orthogonal to a spherical surface $\Sigma$. There are two such congruences, which we may call inward and outward directed. Let us denote by $\Theta_{in}$ and $\Theta_{out}$ their respective expansion. In flat space, $\Theta_{in} < 0$, while $\Theta_{out} > 0$. Surfaces $\Sigma$ with this property are called "normal". If both expansions are negative, the surface is called "trapped", while if both are positive, the surface is "anti-trapped". In terms of the MS variables [13], we have

$$\Theta_{in} = \frac{2}{R}(U - \Gamma) \quad \text{and} \quad \Theta_{out} = \frac{2}{R}(U + \Gamma). \tag{22}$$

In a spherically symmetric spacetime, any point in the $(r, t)$ plane can be thought of as a closed surface $\Sigma$ of proper radius $R(r, t)$. We can classify such points into normal, trapped and anti-trapped. In the transition from a normal region to a trapped region, we must go through a boundary where $\Theta_{in} < 0$ and $\Theta_{out} = 0$. This is a marginally trapped surface which is usually called the apparent horizon. Since $\Theta_{in}\Theta_{out} \propto U^2 - \Gamma^2 = 0$ and using Eq. (4), the condition for the formation of an apparent horizon is simply

$$R = 2M. \tag{23}$$

This could be marginally trapped, as it occurs for black holes, or marginally anti-trapped, as is the case for a cosmological horizon. If the condition $R < 2M$ is satisfied in the vicinity of the apparent horizon, this means that we have trapped surfaces, and a PBH will be formed in the subsequent evolution.

## VI. RESULTS

All variables in the following section are in units of the initial time $t_i = 1$. Numerical simulations are performed by using 95 Chebyshev grid points for the r-axis, with $0 \leq r \leq 200$. The range of $r$ is large enough to keep the formation of the PBH far from the boundaries. We consider an initial wavelength such that the maximum of the initial compaction function is at $r_m = 20$ for the Gaussian case, and therefore using $r_k = r_m$, we have $\epsilon = 1/HL \approx 0.1$. Hence, the long wavelength approximation is justified. The corresponding scale re-enters the horizon at $t_H = 100$. As boundary conditions we are taking $U = R = M = D_r\rho = 0$ at $r = 0$, and $D_r\rho = 0$ at the final grid point, $r = 200$.

### A. Gaussian curvature perturbation

The time evolution of the peaks of the compaction function of the Gaussian profile is given in FIG. 1. At initial time, the compaction function has equally spaced peaks with a very similar amplitude, except for the first one that is slightly larger, and is the maximum of the compaction function. Over time, we can appreciate that the secondary peaks dissipate and eventually disappear while the first maximum moves towards the center of symmetry while it grows. In FIG. 2, we show the difference $(2M - R)$. Normal surfaces satisfy $R > 2M$, while trapped surfaces satisfies $R < 2M$. When $R = 2M$, the apparent horizon is formed, signaling the onset of gravitational collapse. In this particular case, with $f_{NL} = 0$, the apparent horizon is already formed for an amplitude $\mu \approx 0.63$ and thus the corresponding threshold for the compaction function is $\mathcal{C}_{th} \approx 0.30$. Note that the formation of the trapped surface in the limit case happens approximately 16 times after the overdensity has entered in the cosmological horizon $t_H$.

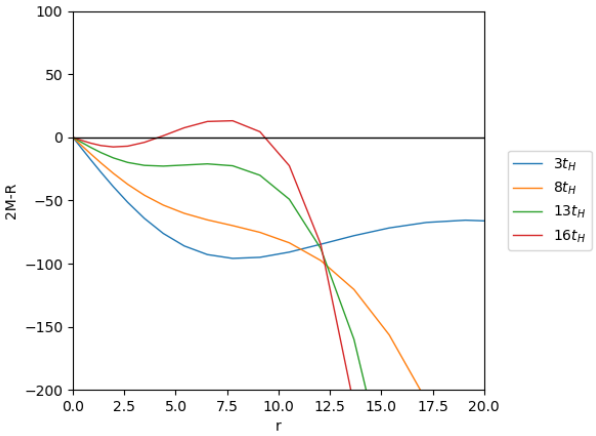


FIG. 2: The difference $(2M - R)$ for the Gaussian profile with $\mu = 0.64$ is plotted for different moments in time as a function of $r$. The condition $2M - R < 0$ implies that we have normal surfaces, while $2M - R > 0$ implies trapped surfaces. The transition point where $2M = R$ is a marginally trapped surface or apparent horizon.

### B. The effect of local non-Gaussianity

To estimate the effect of local non-Gaussianity, we have determined the threshold amplitude $\mu_{th}$ and the threshold compaction function $\mathcal{C}_{th}$ for different values of the non-Gaussianity parameter $f_{NL}$, in the range $-0.5 \leq f_{NL} \leq 6$. The results are shown in FIG. 3. As expected, the value of $C_{th}$ has only a rather modest variability. This is expected, since this threshold value has to be within the bounds given in Eq. (21). This is the reason that makes $\mathcal{C}$ a rather robust estimator of the strength of a perturbation. Actually, the minimum threshold that we find in our one parameter family of non-Gaussian profiles is approximately 0.28, for $f_{NL} \approx 1.7$. This does not even saturate the minimum possible value $\mathcal{C}_{th} \approx 0.21$ which can be obtained with more general profiles. On the other hand, the maximum threshold value $\mathcal{C}_{th} = 1/3$ seems to be within the family for negative values of $f_{NL}$. Unfortunately, however, for

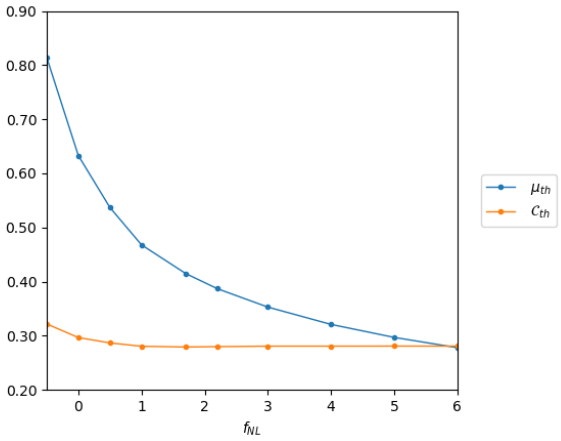


FIG. 3: The threshold values $\mu_{th}$ and $\mathcal{C}_{th}$ are plotted as a function of the local non-Gaussianity parameter $f_{NL}$. While $C_{th}$ is almost independent of $f_{NL}$, we find that $\mu_{th}$ varies quite significantly.

$f_{NL} < -0.5$ our numerical simulation becomes unstable and the calculation is interrupted before the black hole could be formed, so we did not explore smaller values of $f_{NL}$. This is left for further study. By contrast with $\mathcal{C}_{th}$, we find that the threshold amplitude $\mu_{th}$, which is needed for the formation of a PBH, decreases quite significantly with the increase of the non-Gaussianity parameter $f_{NL}$, from $\mu_{th} \approx 0.81$ for $f_{NL} = -0.5$ to its minimum $\mu_{th} \approx 0.28$ for $f_{NL} = 6$. Consequently, the probability of PBH formation, $\mathcal{P} \propto \exp\left(-\frac{\mu_{th}^2}{2\sigma_0^2}\right)$, is enhanced very significantly for profiles with $f_{NL} > 0$, since a smaller threshold $\mu_{th}$ for the amplitude triggers gravitational collapse.

## VII. SUMMARY AND CONCLUSIONS

Primordial black holes may be formed in the radiation dominated era when superhorizon cosmological perturbations $\zeta$ re-enter the horizon with a sufficiently large amplitude, to continue growing until a trapped surface is formed. The abundance of PBH is determined by the power spectrum $P_\zeta(k)$, which should be enhanced at the PBH scale $k_0$. Here, the power spectrum has been modelled by a $\delta$ function in momentum space. This leads us to high peaks of $\zeta(r)$ with a typical profile which is nearly spherically symmetric, and of the form given in Eq. (17) (for the Gaussian case). Inflationary models with a sharp enhancement in the power spectrum usually give rise to local non-Gaussianity in the distribution of $\zeta$. In this work, we have shown that this can significantly affect the probability of PBH formation. Through numerical simulation, we have determined the threshold amplitude $\mu_{th}$ of the high peak profiles for different values of the local non-Gaussianity parameter $0.5 \leq f_{NL} \leq 6$. This can vary substantially, by a factor of order 3 in this range. Since the probability of PBH formation is proportional to $\exp(-\mu_{th}^2/2\sigma_0^2)$, we conclude that PBH formation is more likely for larger values of the non-Gaussianity parameter $f_{NL}$, since smaller values of $\mu_{th}$ are needed for the gravitational collapse to take place. We have also computed the corresponding threshold values $\mathcal{C}_{th}$ for the compaction function, which turn out to be fairly insensitive to $f_{NL}$. This confirms that the compaction function is a quite robust estimator of the strength of density perturbations. In particular, it saturates to a constant value 0.28 for $f_{NL} \gtrsim 1$. This can be used, for instance, in order to find $\mu_{th}$ for any $f_{NL} \gtrsim 2$ without the need of running additional simulations.

### Acknowledgments

I would specially like to thank J. Garriga and V. Atal for all the time and dedication, without their guidance this work would never have been possible. Also, I would like to thank A. Escrivà for sharing his work and his willingness to help. Finally, a mention to my family and friends for their never ending support.

[1] S. Hawking, Mon. Not. Roy. Astron. Soc. **152**, 75 (1971).
[2] B. J. Carr and S. W. Hawking, Mon. Not. Roy. Astron. Soc. **168**, 399 (1974).
[3] M. Sasaki, T. Suyama, T. Tanaka and S. Yokoyama, Class. Quant. Grav. **35**, no.6, 063001, (2018).
[4] V. Atal, J. Garriga and A. Marcos-Caballero, arXiv:1905.13202 [astro-ph.CO].
[5] M. Shibata and M. Sasaki, Phys. Rev. D **60**, 084002, (1999).
[6] R. Penrose, Phys. Rev. Lett. **14**, 57 (1965).
[7] A. Escrivà, "Numerical simulation of primordial black hole formation using spectral methods", in preparation.
[8] C. W. Misner and D. H. Sharp, **136**, B571 (1964).
[9] V. Mukhanov, "Physical Foundations of Cosmology,", Cambridge University Press, New York (2005).
[10] I. Musco, arXiv:1809.02127 [gr-qc].
[11] J. M. Bardeen, J. R. Bond, N. Kaiser and A. S. Szalay, Astrophys. J. **304**, 15 (1986). doi:10.1086/164143.
[12] M. Kopp, S. Hofmann and J. Weller, Phys. Rev. D **83**, 124025 (2011) doi:10.1103/PhysRevD.83.124025 [arXiv:1012.4369 [astro-ph.CO]].
[13] A. Helou, I. Musco and J. C. Miller, Class. Quant. Grav. **34**, 135012, (2017).